

---

# Alchemy: A benchmark and analysis toolkit for meta-reinforcement learning agents

---

Jane X. Wang<sup>\*†1</sup>, Michael King<sup>\*1</sup>, Nicolas Porcel<sup>1</sup>, Zeb Kurth-Nelson<sup>1,2</sup>,  
Tina Zhu<sup>1</sup>, Charlie Deck<sup>1</sup>, Peter Choy<sup>1</sup>, Mary Cassin<sup>1</sup>, Malcolm Reynolds<sup>1</sup>,  
Francis Song<sup>1</sup>, Gavin Buttimore<sup>1</sup>, David P. Reichert<sup>1</sup>, Neil Rabinowitz<sup>1</sup>,  
Loic Matthey<sup>1</sup>, Demis Hassabis<sup>1</sup>, Alexander Lerchner<sup>1</sup>, Matthew Botvinick<sup>‡1,2</sup>

<sup>1</sup>DeepMind, London, UK

<sup>2</sup>University College London, London, UK

## Abstract

There has been rapidly growing interest in meta-learning as a method for increasing the flexibility and sample efficiency of reinforcement learning. One problem in this area of research, however, has been a scarcity of adequate benchmark tasks. In general, the structure underlying past benchmarks has either been too simple to be inherently interesting, or too ill-defined to support principled analysis. In the present work, we introduce a new benchmark for meta-RL research, emphasizing transparency and potential for in-depth analysis as well as structural richness. Alchemy is a 3D video game, implemented in Unity, which involves a latent causal structure that is resampled procedurally from episode to episode, affording structure learning, online inference, hypothesis testing and action sequencing based on abstract domain knowledge. We evaluate a pair of powerful RL agents on Alchemy and present an in-depth analysis of one of these agents. Results clearly indicate a frank and specific failure of meta-learning, providing validation for Alchemy as a challenging benchmark for meta-RL. Concurrent with this report, we are releasing Alchemy as public resource, together with a suite of analysis tools and sample agent trajectories.

## 1 Introduction

Techniques for deep reinforcement learning have matured rapidly over the last few years, yielding high levels of performance in tasks ranging from chess and Go [53] to realtime strategy [66, 42] to first person 3D games [28, 69]. However, despite these successes, poor sample efficiency, generalization, and transfer remain widely acknowledged pitfalls. To address those challenges, there has recently been growing interest in the topic of meta-learning [7, 64], and how meta-learning abilities can be integrated into deep RL agents [67, 6]. Although a bevy of interesting and innovative techniques for meta-reinforcement learning have been proposed [e.g., 19, 71, 47, 57], research in this area has been hindered by a ‘problem problem,’ that is, a dearth of ideal task benchmarks. In the present work, we contribute toward a remedy, by introducing and publicly releasing a new and principled benchmark for meta-RL research.

Where deep RL requires a task, meta-RL instead requires a *task distribution*, a large set of tasks with some form of shared structure. Meta-RL is then defined as any process that yields faster learning, on average, with each new draw from the task distribution [60, 51, 5]. A straightforward way to

---

\*Equal contribution

†Correspondence to: wangjane@google.com

‡Correspondence to: botvinick@google.com

generalize the problem setting is in terms of an underspecified partially observable Markov decision problem [UPOMDP; 13]. This enriches the standard POMDP tuple  $\langle S, A, \Omega, T, R, O \rangle$ , respectively a set of states, actions, and observations, together with state-transition, reward and observation functions [58], adding a set of parameters  $\Theta$  which govern the latter three functions. Importantly,  $\Theta$  is understood as a random variable, governed by a prior distribution and resulting in a corresponding distribution of POMDPs. In this setting, meta-RL can be viewed in terms of hierarchical Bayesian inference, with a relatively slow process, spanning samples, gradually inferring the structure of the parameterization  $\Theta$ , and in turn supporting a rapid process which infers the specific parameters underlying new draws from the task distribution [43, 23, 15, 1]. In this way, meta-RL is equivalent to latent structure learning, as it is the structure in the tasks that allows for fast adaptation in the inner loop. In black-box approaches to meta-RL, this fast process is active, involving strategic information gathering or experimentation [18, 11]. In the limit of training, such approaches are able to implement Bayes-optimal policies due to their meta-learning objective [39, 43], and analysis of their internal representations shows that they come to represent the task in a similar way to Bayes-optimal agents, capturing the necessary and latent structure of the task family.

This perspective brings into view two further desiderata for any benchmark meta-RL task distribution. First, the ground-truth parameterization of the distribution should ideally be *accessible*. This allows agent performance to be compared directly against an optimal baseline, which is precisely a Bayesian learner, sometimes referred to as an ‘ideal observer’ [20, 43]. Second, the structure of the task distribution should be *interesting*, in that it displays properties comparable to those involved in many challenging real-world tasks. Intuitively, in the limit, interesting structure should feature compositionality, causal relationships, and opportunities for conceptual abstraction [36], and result in tasks whose diagnosis and solutions require strategic sequencing of actions.

Unfortunately, the environments employed in previous meta-RL research have tended to satisfy one of the above desiderata at the expense of the other (see Section 2 on related work). Here, we introduce a task distribution that checks both boxes, offering both accessibility and interestingness, and thus a best-of-both-worlds benchmark for meta-RL research. *Alchemy* is a 3D, first-person perspective video game implemented in the Unity game engine (www.unity.com). It has a highly structured and non-trivial latent causal structure which is resampled every time the game is played, requiring knowledge-based experimentation and strategic action sequencing. Because levels are procedurally created based on a fully accessible, compositional, generative process with well-defined parameterization, we are able to implement a Bayesian ideal observer as a gold standard for performance.

In addition to introducing the Alchemy environment, we evaluate it on two recently introduced, powerful deep RL agents, demonstrating a striking failure of structure learning. Applying a battery of performance probes and analyses to one agent, we provide evidence that its performance reflects a superficial, structure-blind heuristic strategy. Further experiments show that this outcome is not purely due to the sensorimotor complexities of the task, nor to the demands of multi-step decision making. In sum, the limited meta-learning performance appears to be specifically tied to the identification of latent structure, validating the utility of Alchemy as an assay for this particular ability.

## 2 Related work

Where deep RL requires a task, meta-RL instead requires a *task distribution*, a large set of tasks with some form of shared structure. Meta-RL is then defined as any process that yields faster learning, on average, with each new draw from the task distribution [60, 51, 5]. Gradient-based meta-learning approaches such as MAML [19] and variants [e.g., 38, 24, 19] have proven to be quite popular and versatile, but have trouble balancing targeted exploration and exploitation, especially when latent structure is present. Black-box meta-learners, on the other hand, can optimize exploration with exploitation and capitalize on latent task structure to learn efficient exploration end-to-end [68, 14, 50, 40, 56, 27, 73], usually via an autoregressive model such as LSTMs [26] or self-attention [40, 65]. Others have focused on decoupling the exploration issue entirely [37, 47] by learning to predict the task ID, but it remains to be seen if these approaches work when the task distribution has latent structure that is procedurally generated and compositional, as is the case with Alchemy.

A classic example task requiring balanced exploration-exploitation, showcased in studies implementing black-box meta-RL approaches [e.g., 68, 14, 40], is a distribution of bandit problems, each with its own sampled set of action-contingent reward probabilities. Bandits are useful in that they have furnished accessibility, allowing for principled analysis and interpretation of meta-learning performance

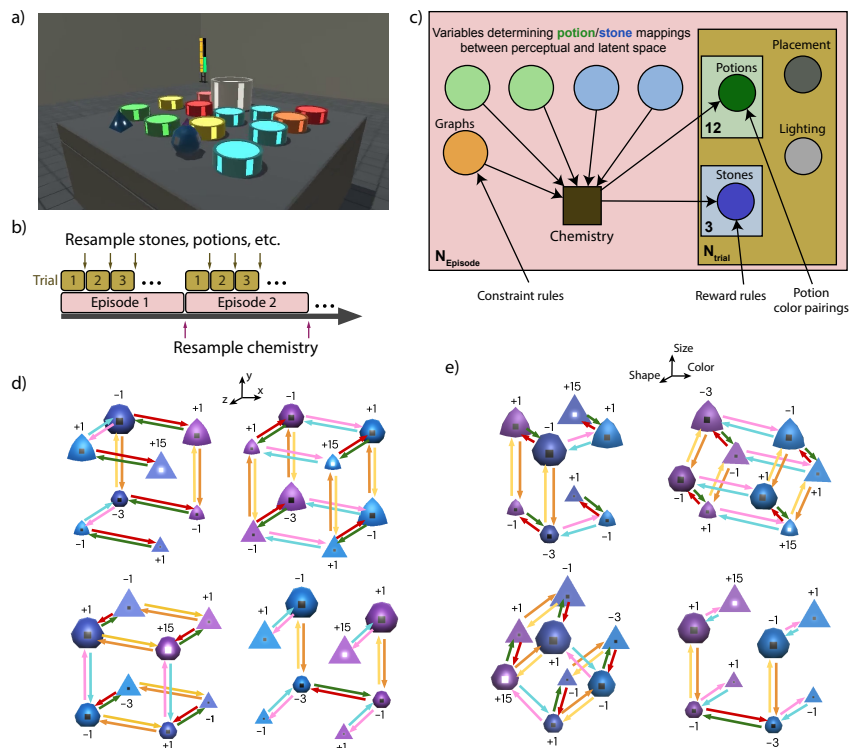


Figure 1: a) Visual observation for Alchemy, RGB, rendered at higher resolution than is received by the agent (96x72). b) Temporal depiction of the generative process, indicating when chemistries and trial-specific instances (stones, potions, placement, lighting) are resampled. c) A high-level depiction of the generative process for sampling a new task, in plate notation. Certain structures are fixed for all episodes, such as the constraint rules governing the possible graphs, the way rewards are calculated from stone latent properties, and the fact that potions are paired into opposites. Every episode, a graph and a set of variables determining the way potions and stones are mapped between latent and perceptual space are sampled to form a new chemistry. Conditioned on this chemistry, for each of  $N_{trial} = 10$  trials,  $N_s = 3$  specific stones and  $N_p = 12$  potions are sampled, as well as random position and lighting conditions, to form the perceptual observation for the agent. See Appendix A.1 and Figure 6 for more details. d) Four example chemistries, in which the latent axes are held constant (worst stone is at the origin). e) The same four chemistries, but with perceptual axes held constant. Note that the edges of the causal graph need not be axis aligned with the perceptual axes.

[68, 14, 43] via comparison with known optimal solutions [see, e.g., 21, 3]. However, they fail on the interestingness front by focusing on very simple task parameterization structures. In Alchemy, we are in a position to compare agent performance against an optimal baseline in the context of a much more interesting – compositional, causal, and conceptual – task distribution. Further, Alchemy was designed with inspiration from cognitive science studies of human behavior [36, 59], where it is argued that latent structure learning is generic to real-world tasks and human-like intelligence. It therefore shares many properties with tasks that evoke human-like cognition, such when children learn to experiment in their environment to learn about causal dependencies [22], or tasks that require theory formation, causal understanding, or planning in a latent space [11, 62]. As with bandits, behavioral tasks in cognitive science also focus on accessibility and understanding, particularly animal tasks, which prioritize interpretability and modeling underlying mechanisms [17, 12] over complexity, and thus are relatively simple [32], especially compared to tasks in AI.

These kinds of properties are notably absent in the most popular meta-RL benchmarks today, which mostly focus on efficient few-shot adaptation of control policies (e.g. MuJoCo continuous control tasks [61, 63] or MetaWorld [72]), in which latent aspects of the task are limited to a single parameter such as goal location. Strategic, smart exploration and latent structure learning are thus not required. At the other end of the spectrum, tasks with more interesting and diverse structure (e.g., Atari [4] or CoinRun [9]) have been grouped together as task distributions, but the underlying structure or

parameterization of those distributions is not transparent [4, 45, 49, 41]. Environments have also been created with emphasis on increasing amounts of complexity and exploration demands, such as NetHack [35], ALFRED [54], Progen [8], DeepMind Lab [2], interfaces to Minecraft [31], and Obstacle Tower [34], often via procedural generation. Training on procedurally generated tasks improves generalization performance [48, 8, 9] by offering high variety and complexity, but at the cost of these tasks being unable to be transparently analyzed. This makes it difficult to know (beyond human intuition) whether a sample from the task distribution supports transfer to further sampled tasks, let alone to construct Bayes-optimal performance baselines for such transfer. Thus, the current state of meta-RL benchmarks is focused primarily on either efficient adaptation, or enhancing complexity and exploration, at the cost of comprehensibility. Alchemy is distinguished in the compositional and latent structure in which it’s procedurally generated, in a manner amenable to analysis—similar to bandits, but more complex—and is focused on latent structure learning. However, we note that we are not the first to emphasize interpretability and diagnosis of certain skills [70, 44, 25], and hope to see more benchmarks emerge with this same philosophy.

### 3 The Alchemy environment

Alchemy is a 3D environment created in Unity [33], played in a series of ‘trials’, which fit together into ‘episodes.’ Within each trial, the goal is to use a set of potions to transform each in a collection of visually distinctive stones into more valuable forms, collecting points when the stones are dropped into a central cauldron. The value of each stone is tied to its perceptual features, but this relationship changes from episode to episode, as do the potions’ transformative effects. Together, these structural aspects of the task constitute a ‘chemistry’ that is fixed across trials within an episode, but resampled at the start of each episode, based on a highly structured, compositional, generative process (see Figure 1). The implicit challenge within each episode is thus to diagnose, within the available time, the current chemistry, leveraging this diagnosis to manufacture the most valuable stones possible.

#### 3.1 Observations, actions, and task logic

At the beginning of each trial, the agent views a table containing a cauldron together with three stones and twelve potions, as sampled from Alchemy’s generative process (Figure 1a). Stone appearance varies along three feature dimensions: size, color and shape. Each stone also displays a marker whose brightness signals its point value (-3, -1, +1 or +15). Each potion appears in one of six hues. The agent receives 96x72 RGB pixel observations from an egocentric perspective, together with proprioceptive information (acceleration, distance of and force on the hand, and whether the hand is grasping an object). It selects actions from a nine-dimensional set (consisting of navigation, object manipulation actuators, and a discrete *grab* action). When a stone comes into contact with a potion, the latter is consumed and, depending on the current chemistry, the stone appearance and value may change. Each trial lasts sixty seconds, simulated at 30 frames per second. A visual indicator in each corner of the workspace indicates time remaining. Each episode comprises ten trials, with the chemistry fixed across trials but stone and potion instances, spatial positions, and lighting resampled at the onset of each trial (Figure 1b). See <https://youtu.be/k2ziWeyMxAk> for a game play video.

#### 3.2 The chemistry

As noted earlier, the causal structure of the task changes across episodes. The current ‘chemistry’ determines the particular stone appearances that can occur, the value attached to each appearance, and, crucially, the transformative effects that potions have on stones. The specific chemistry for each episode is sampled from a structured generative process, illustrated in Figure 1c-e and fully described in the Appendix. For brevity, we limit ourselves here to a high-level description.

To foreground the meta-learning challenge involved in Alchemy, it is useful to distinguish between (1) the aspects of the task that can change across episodes and (2) the abstract principles or regularities that span all episodes. As we have noted, the former, changeable aspects include stone appearances, stone values, and potion effects. Given all possible combinations of these factors, there exist a total of 167,424 possible chemistries (taking into account that stone and potion instances are also sampled per trial yields a total set of possible trial initializations on the order of 124 billion, still neglecting variability in the spatial positioning of objects, lighting, etc).<sup>4</sup> The principles that span episodes are, in a sense, more important, since identifying and exploiting these regularities is the essence of the

<sup>4</sup>Note that this corresponds to the sample space for the parameter set  $\Theta$  mentioned in the Introduction.

meta-learning problem. The invariances that characterize the generative process in Alchemy can be summarized as follows:

1. Within each episode, stones with the same visual features have the same value and respond identically to potions. Analogously, potions of the same color have the same effects.
2. Within each episode, only eight stone appearances can occur, and these correspond to the vertices of a cube in the three-dimensional appearance space. Potion effects run only along the edges of this cube, effectively making it a causal graph.
3. Each potion type (color) ‘moves’ stone appearances in only one direction in appearance space. That is, each potion operates only along parallel edges of the cubic causal graph.
4. Potions come in fixed pairs (red/green, yellow/orange, pink/turquoise) which always have opposite effects. The effect of the red potion, for example, varies across episodes, but whatever its effects, the green potion will have the converse effects.
5. In some chemistries, edges of the causal graph may be missing, i.e., no single potion will effect a transition between two particular stone appearances.<sup>5</sup> However, the topology of the underlying causal graph is not arbitrary; it is governed by a generative grammar that yields a highly structured distribution of topologies (see Appendix A.1 and Figure 7).

These conceptual aspects of the task remain invariant across episodes, so experience gathered from a large set of episodes affords the opportunity for an agent to discover them, tuning into the structure of the generative process giving rise to each episode and trial. It is the ability to learn at this level, and to exploit what it learns, that corresponds to an agent’s meta-learning performance.

### 3.3 Symbolic version

As a complement to the canonical 3D version of Alchemy, we have also created a symbolic version of the task. This involves the same underlying generative process and preserves the challenge of reasoning and planning over the resulting latent structure, but factors out the visuospatial and motor complexities of the full environment. Symbolic Alchemy returns as observation a concatenated vector indicating the features of all sampled potions and stones, and entails a discrete action space, specifying a stone and a container (either potion or cauldron) in which to place it, plus a *no-op* action (navigation is not required). Full details are presented in the Appendix.

### 3.4 Ideal-observer reference agent

AGENT	EPISODE SCORE
IMPALA	140.2 ± 1.5
VMPO	156.2 ± 1.6
VMPO (SYMBOLIC)	155.4 ± 1.6
IDEAL OBSERVER	284.4 ± 1.6
ORACLE	288.5 ± 1.5
RANDOM HEURISTIC	145.7 ± 1.5

Table 1: Benchmark and baseline-agent evaluation scores (mean ± standard error over 1000 episodes).

end of the current trial. The resulting policy both marks out the highest attainable task score (in expectation) and exposes minimum-regret action sequences, which optimally balance exploration or experimentation against exploitation.<sup>6</sup> Any agent matching the score of the ideal observer

As noted in the Introduction, when a task distribution is fully accessible, this makes it possible to construct a Bayes-optimal ‘ideal observer’ reference agent as a gold standard for evaluating the meta-learning performance of any agent. We constructed just such an agent for Alchemy, as detailed in the Appendix (Algorithm 1). This agent maintains a belief state over all possible chemistries given the history of observations, and performs an exhaustive search over both available actions (as discretized in symbolic Alchemy) and possible outcomes in order to maximize reward at the

<sup>5</sup>When this is the case, in order to anticipate the effect of some potions the player must attend to conjunctions of perceptual features. Missing edges can also create bottlenecks in the causal graph, which make it necessary to first transform a stone to look *less* similar to a goal appearance before it is feasible to attain that goal state.

<sup>6</sup>Our ideal observer does not account for optimal inference over the entire length of the episode, which would be computationally intractable to calculate. However, in general, we find that a single trial is enough to narrow down the number of possible world states to a much smaller number, and thus searching for more than one trial does not confer significant benefits.

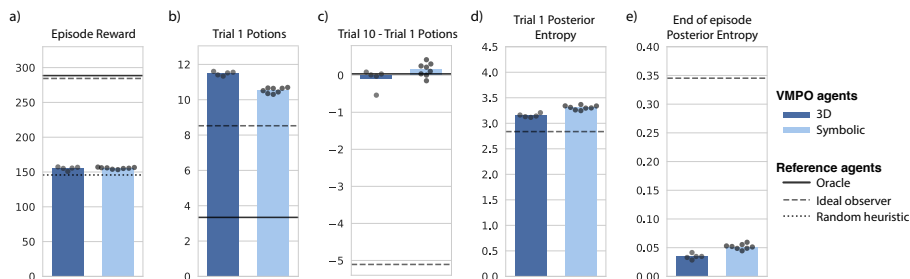


Figure 2: Detailed analysis of behavior of VMPO agents on 1000 evaluation episodes in 3D Alchemy and symbolic Alchemy, in comparison with the reference agents which have been handcrafted with specific knowledge (oracle, Bayesian ideal observer, and random heuristic). a) Episode reward. b) Number of potions used in Trial 1. c) Difference between number of potions used in trial 10 vs trial 1. d) Posterior entropy over world states, conditioned on agent actions, at end of trial 1. e) Posterior entropy over world states at the end of the episode. Filled black circles indicate individual replicas (5-8 per condition). Note that the oracle and random heuristic reference agents don’t maintain a belief state and thus are not indicated in d-e.

demonstrates, in doing so, both a thorough understanding of Alchemy’s task structure and strong action-sequencing abilities.

As further tools for analysis, we devised two other reference agents. An *oracle* reference agent is given privileged access to a full description of the current chemistry, and performs a brute-force search over the available actions, seeking to maximizing reward (see Appendix, Algorithm 2). A *random heuristic* reference agent chooses a stone at random, using potions at random until that stone reaches the maximum value of +15 points. It then deposits the stone in the cauldron, and repeats with a new one (Appendix, Algorithm 3). The resulting policy yields a score reflecting what is possible in the absence of any guiding understanding of the latent structure of the Alchemy task.

## 4 Experiments

### 4.1 Agent architectures and training

**VMPO agent:** As described in [55] and [46], this agent centered on a gated transformer XL network. Image-frame observations were passed through a residual-network encoder and fully connected layer, with proprioceptive observations, previous action and reward then concatenated. In the symbolic task, observations were passed directly to the transformer core. Losses were included for policy and value heads, pixel control [30], kickstarting [52, 10] and latent state prediction (see Section 4.3). Where kickstarting was used (see below), the loss was  $KL(\pi_{student} || \pi_{teacher})$ , and the weighting was set to 0 after  $5e8$  steps. Further details are presented in Appendix Table 2.

**IMPALA agent:** This agent is described by [16], and used population-based training as presented by [29]. Pixel observations passed through a residual-network encoder and fully connected layer, and proprioceptive observations were concatenated to the input at every spatial location before each residual-network block. The output was fed into the core of the network, an LSTM.<sup>7</sup> Pixel control and kickstarting losses were used, as in the VMPO agent. See Appendix Table 3 for details.

Both agents were trained for  $2e10$  steps ( $4.44e6$  training episodes;  $1e9$  episodes for the symbolic version of the task), and evaluated without weight updates on 1000 test episodes. Note that to surpass a zero score in full, 3D, image-based Alchemy, both agents required kickstarting [52], with agents first trained on a fixed chemistry with shaping rewards included for each potion use. Agents trained on the symbolic version of the task were trained from scratch without kickstarting.

### 4.2 Agent performance and diagnostic analyses

Mean episode scores for both agents are shown in Table 1. Both fell far short of the gold-standard ideal observer benchmark, implying a failure of meta-learning. In fact, scores for both agents fell close to that attained by the random heuristic reference policy. In order to better understand these results,

<sup>7</sup>Recurrent state was set to zero at episode boundaries, but not between trials, enabling the agents (in principle) to utilise knowledge of the chemistry accumulated over previous trials.

we conducted a series of additional analyses, focusing on the VMPO agent given its slightly higher baseline score. These analyses are based on a principle of progressively allowing the agent access to different forms of privileged information about the environment in order to pinpoint the source of difficulty. Importantly, note that having access to these kinds of information is not considered ‘solving’ *Alchemy*, but rather is merely diagnostic of the specific limitations of current agents, which are falling short in ways we detail below.

A first question was whether this agent’s poor performance is due either to the difficulty of discerning task structure through the complexity of high-dimensional pixel observations, or to the challenge of sequencing actions in order to capitalize on inferences concerning the task’s latent state. A clear answer is provided by the scores from a VMPO agent trained and tested on the symbolic version of *Alchemy*, which lifts both of these challenges while continuing to impose the task’s more fundamental requirement for structure learning and latent-state inference. As shown in Table 1 and Figure 2a, performance was no better in this setting than in the canonical version of the task, again only slightly surpassing the score from the random heuristic policy.

Informal inspection of trajectories from the symbolic version of the task was consistent with the conclusion that the agent, like the random heuristic policy, was dipping stones in potions essentially at random until a high point value happened to be attained. To test this impression more rigorously, we measured how many potions the agent consumed, on average, during the first and last trials within an episode. As shown in Figure 2b, the agent used more potions during episode-initial trials than the ideal observer benchmark. From Figure 2c, we can see that the ideal observer used a smaller number of potions in the episode-final trial than in the initial trial, while the VMPO baseline agent showed no such reduction (see Appendix Figure 10 for more detailed results). By selecting diagnostic actions, the ideal observer progressively reduces its uncertainty over the current latent state of the task (i.e., the set of chemistries possibly currently in effect, given the history of observations). This is shown in Figure 2d-e, in units of posterior entropy, calculated as the log of the number of states still possible, according to the ideal observer. The VMPO agent’s actions also effectively reveal the chemistry, as indicated in the figure. The fact that the agent is nonetheless scoring poorly and overusing potions implies that it is failing to make use of the information its actions have inadvertently revealed about the task’s latent state.

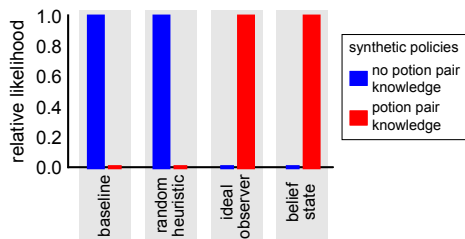


Figure 3: Bayesian model comparison. Two synthetic, probabilistic policies were crafted and compared with the actions of VMPO and reference agents: (1) a policy that does not assume potions come in pairs with opposite effects (blue bars), and (2) a policy that does (red bars). Comparing the goodness of fit between these policies, we found that both the baseline VMPO agent and the random heuristic were better fit by model (1), while the VMPO agent which had belief state extra input was better fit by model (2), and thus appeared to exploit knowledge of potion pairs.

shown in Figure 3, when the predictions of these two policies were compared to the actions of the ideal observer reference agent, in terms of relative likelihood, results clearly indicated a superior fit for the policy leveraging knowledge of the potion pairings. In contrast, for the random heuristic

The behavior of the VMPO agent suggests that it has not tuned into the consistent principles that span chemistries in *Alchemy*, as enumerated in Section 3.2. One way of probing the agent’s ‘understanding’ of individual principles is to test how well its behavior is fit by synthetic, adaptive, probabilistic policies that either do or do not leverage one relevant aspect of the task’s structure, a technique frequently used in cognitive science to analyze human learning and decision making [12, 17]. We applied this strategy to evaluate whether agents trained on the symbolic version of *Alchemy* was leveraging the fact that potions come in consistent pairs with opposite effects (see Section 3.2). Two hand-crafted, probabilistic policies were devised, both of which performed single-step look-ahead to predict the outcome (stones and potions remaining) for each currently available action, attaching to each outcome a value equal to the sum of point-values for stones present, and selecting the subsequent action based on a soft-max over the resulting state values. In both policies, predictions were based on a posterior distribution over the current chemistry. However, in one policy this posterior was updated with built-in knowledge of the potion pairings, while the other policy ignored this regularity of the task. As

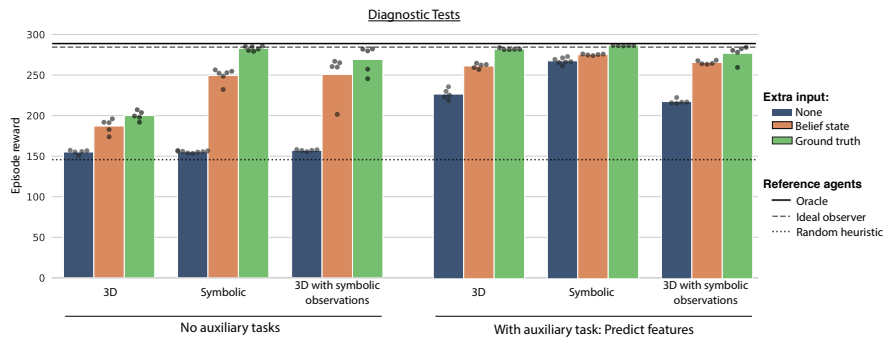


Figure 4: Evaluation performance of VMPO agents under additional diagnostic conditions (not considered part of the Alchemy benchmark). Orange bars add extra input with belief state of ideal observer. Green bars add extra input with ground truth chemistry knowledge. In "3D with symbolic observations" condition, agent acts in 3D world, but is also given the observations it would receive in the corresponding configuration of the symbolic task. Finally, the right group of 9 bars adds an auxiliary feature prediction task. Filled black circles indicate individual replicas (5-8 per condition).

reference agent, a much better fit was attained for the policy operating in ignorance of the pairings. Applying the same analysis to the behavior of the baseline VMPO agent yielded results mirroring those for the random heuristic agent (see Figure 3 'baseline'), consistent with the conclusion that the VMPO agent's policy made no strategic use of the existence of consistent relationships between the potions' effects.

### 4.3 Augmentation studies

A standard strategy in reinforcement learning research is analyzing the operation of a performant agent via a set of ablations, to determine what factors are causal in the agent's success. Confronted with a poorly performing agent, we inverted this strategy, undertaking a set of *augmentations* (additions to either the task or the agent) in order to identify what factors might be holding the agent back.

Given the failure of the VMPO agent to show signs of identifying the latent structure of the Alchemy task, one question of clear interest is whether performance would improve if the task's latent state were rendered observable. In order to study this, we trained and tested on a version of symbolic Alchemy which supplemented the agent's observations with a binary vector indicating the complete current chemistry (see Appendix for details). When furnished with this additional information, the agent's average score jumped dramatically, landing very near the score attained by the ideal observer reference (Figure 4 'Symbolic', 'Extra input: Ground truth'). Note that this augmentation gives the agent privileged access to an oracle-like indication of the current ground-truth chemistry. In a less drastic augmentation, we replaced this additional input with a vector indicating not the ground-truth chemistry, but instead the set of chemistries consistent with observations made so far in the episode, corresponding to the Bayesian belief state of the ideal observer reference model ('Extra input: Belief state'). While the resulting scores in this setting were not quite as high as those in the ground-truth augmentation experiment, they were much higher than those observed without augmentation (i.e. 'Extra input: None'). Furthermore, the agent furnished with the belief state resembled the ideal observer agent in showing a clear reduction in potion use between the first and last trials in an episode (Figure 5a-b).<sup>8</sup> Model fits also indicated the agent receiving this input made use of the opposite-effects pairings of potions, an ability not seen in the baseline VMPO agent (Figure 3).

The impact of augmenting the input with an explicit representation of the chemistry implies that the VMPO agent, while evidently unable to identify Alchemy's latent structure, can act adaptively if that latent structure is helpfully brought to the surface. Since this observation was made in the setting of the symbolic version of Alchemy, we tested the same question in the full 3D version of the task. Interestingly, the results here were somewhat different: While appending a representation of either the ground-truth chemistry or belief state to the agent's observations did increase scores, the effect

<sup>8</sup>In contrast, when the agent was furnished with the full ground truth, it neither reduced its potion use over time nor so effectively narrowed down the set of possible chemistries. This makes sense, however, given that full knowledge of the current chemistry allows the agent to be highly efficient in potion use from the start of the episode, and relieves it from having to perform diagnostic actions to uncover the current latent state.

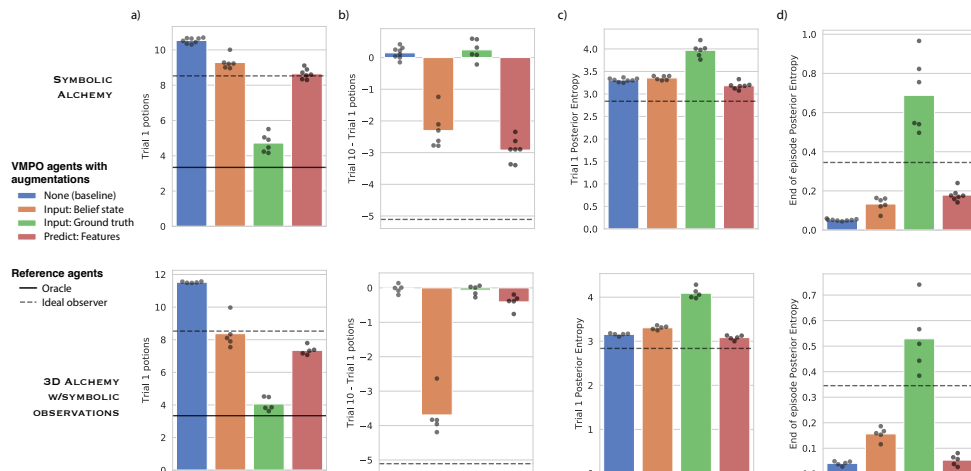


Figure 5: Behavioral metrics for agents trained under different diagnostic conditions and augmentations in symbolic alchemy (top) and 3D alchemy with symbolic observations (bottom). a) Number of potions used in Trial 1. b) Difference between number of potions used in trial 10 vs trial 1. c) Posterior entropy over world states, conditioned on agent actions, at end of trial 1. d) Posterior entropy over world states at the end of the episode. Filled black circles are individual replicas.

was not as categorical as in the symbolic setting (Figure 4 ‘3D’). Two hypotheses suggest themselves as explanations for this result. First, the VMPO agent might have more trouble capitalizing on the extra information in the 3D version of Alchemy because doing so requires composing much longer sequences of action than does the symbolic version of the task (due to the need to navigate around in a 3D environment). Second, the greater complexity of the agent’s perceptual observations might make it harder to map this extra information onto the structure of its current perceptual inputs. As one step toward adjudicating between these possibilities, we augmented the inputs to the agent in the 3D task with the observations that the symbolic version of the task would provide in the same state. In the absence of extra input about the currently prevailing chemistry, this augmentation did not change the agent’s behavior; the resulting score still fell close to the random reference policy (Figure 4 ‘3D with symbolic observations’). However, adding either the ground-truth or belief-state input raised scores much more dramatically than when those inputs were included without symbolic state information, elevating them to levels comparable to those attained in the symbolic task itself and approaching the ideal observer model, with parallel effects on potion use (Figure 5a-b). These results suggest that the failure of the agent to fully utilize this extra information about the current chemistry was not due to challenges of action sequencing in the full 3D version of Alchemy, but stemmed instead from an inability to effectively map such information onto internal representations of the current perceptual observation.

While augmenting the agent’s inputs is one way to impact its representation of current visual inputs, the recent deep RL literature suggests a different method for enriching internal representations, which is to add auxiliary tasks to the agent’s training objective [see, e.g., 30]. As one application of this idea, we added to the RL objective a set of supervised tasks, the objectives of which were to produce outputs indicating (1) the total number of stones present in each of a set of perceptual categories, (2) the total number of potions present of each color, and (3) the currently prevailing ground-truth chemistry (see Appendix B.2 for further details).<sup>9</sup>

Introducing these auxiliary tasks had a dramatic impact on agent performance, especially for (1) and (2) (less so for (3), see Figure 9 in Appendix). This was true even in the absence of extra belief-state or ground-truth input, but the most dramatic benefits were achieved when both forms of augmentation were present, yielding the highest scores observed so far in the full 3D version of Alchemy (Figure 4 ‘3D’). Indeed, in the presence of the auxiliary tasks, further supplementing the inputs with the symbolic version of the perceptual observations added little to agent performance (Figure 4 ‘3D with symbolic observations’). Adding the auxiliary tasks to the objective in symbolic

<sup>9</sup>Prediction tasks (1) and (2) were always done in conjunction and are collectively referred to as ‘Predict: Features’, while (3) is referred to as ‘Predict: Chemistry’.

Alchemy had a striking effect on scores even in the absence of any other augmentation. In this case, scores approached the ideal observer benchmark (Figure 4 ‘Symbolic’), providing the only case in the present study where agents showed respectable meta-learning performance on either version of Alchemy without privileged information at test.<sup>10</sup>

## 5 Discussion

We have introduced Alchemy, a new benchmark task environment for meta-RL research. Alchemy is novel among existing benchmarks in bringing together two desirable features: (1) structural *interestingness*, due to its abstract, causal, and compositional latent organization, which demands experimentation, structured inference and strategic action sequencing; and (2) structural *accessibility*, conferred by its explicitly defined generative process, which furnishes an interpretable prior and supports construction of a Bayes-optimal reference policy, alongside many other analytical maneuvers. With the hope that Alchemy will be useful to the larger community, we are releasing, open-source, both the full 3D and symbolic versions of the Alchemy environment, along with a suite of benchmark policies, analysis tools, and episode logs ([https://github.com/deepmind/dm\\_alchemy](https://github.com/deepmind/dm_alchemy)).

As a first application and validation of Alchemy, we tested two strong deep RL agents which are considered highly performant [16, 46, 55]. In both cases, despite mastering the basic mechanical aspects of the task, neither agent showed any appreciable signs of meta-learning (i.e. structure learning or latent-state inference), which we ascertained through a series of analyses made possible by the task’s accessible structure and comparison with reference agents. Leveraging a symbolic version of Alchemy, we were able to establish that this failure of meta-learning is not due purely to the visual complexity of the task or to the number of actions required to achieve task goals. Finally, a series of augmentation studies showed that deep RL agents can in fact perform well if the latent structure of the task is rendered fully observable, especially if auxiliary tasks are introduced to support representation learning. These insights may, we hope, be useful in developing deep RL agents that are capable of solving Alchemy without access to privileged information. Due to the depth of analysis, this work was limited in only thoroughly characterizing the behavior of one deep RL agent (VMPO). Future work is needed to apply the same level of careful analysis across a broader range of deep RL agents, although we’re hopeful that with the release of this environment and analysis tools, other researchers will find it relatively easy to train and analyze their own agents.

Alchemy is, admittedly, specific in its construction, and therefore limited in terms of its complexity, relative to real-world or other tasks. This was necessary in order to preserve its accessibility, but reduces its ability to challenge agents along other dimensions (such as extended exploration). Another limitation is that extended training can be required, especially for the 3D version. It was necessary to use kickstarting from simpler, reward-shaped versions of the task in order to gain enough signal to overcome the visuomotor difficulties. Due to Alchemy’s partial observability, even the symbolic version can be quite challenging (although it is possible to significantly simplify the environment by holding fixed various aspects of the generative chemistry).

We note that Alchemy is not simply a benchmark to evaluate performance, but a comprehensive analysis suite to help characterize behavior and pinpoint points of failure. We demonstrate a range of detailed, hypothesis-driven, and informative analyses enabled by this testbed, focusing on depth rather than breadth, in order to showcase the extent of what is possible. This is a distinctly cognitive science style of analysis, and is in contrast with performance-focused benchmarks which offer limited potential for analysis or insight into agent behavior (although we are encouraged to see the emergence of new cognitive science-inspired works such as [70]). Importantly, in our view, the main contributions of the present work inhere not in the specific concrete details of Alchemy itself, but rather in the overall scientific agenda and approach. Ascertaining the level of knowledge possessed by deep RL agents is a challenging task, comparable to trying to ascertain the knowledge of real animals, and (as in that latter case) requiring detailed cognitive modeling. Alchemy is designed to make this kind of modeling not only possible, but even central, and we propose that more meta-RL environments should strive to afford the same granularity of insight into agent behavior. As a closing remark, we have found that many humans find playing Alchemy interesting and challenging, and our informal tests suggest that motivated players, with sufficient training, can attain to sophisticated strategies and high levels of performance. Based on this, we suggest that Alchemy may also be an interesting task for research into human learning and decision making.

---

<sup>10</sup>Potion use, as well as world state uncertainty, also showed a reduction over trials (see Figure 5).

## Acknowledgments and Disclosure of Funding

We would like to thank the DeepMind Worlds team – in particular, Ricardo Barreira, Kieran Connell, Tom Ward, Manuel Sanchez, Mimi Jasarevic, and Jason Sanmiya for help with releasing the environment and testing, and Sarah York for her help on testing and gathering human benchmarks. We also are grateful to Sam Gershman, Murray Shanahan, Irina Higgins, Christopher Summerfield, Jessica Hamrick, David Raposo, Laurent Sartran, Razvan Pascanu, Alex Cullum, and Victoria Langston for valuable advisement, discussions, feedback, and support. This work was funded by DeepMind.

## References

- [1] Jonathan Baxter. Theoretical models of learning to learn. In *Learning to learn*, pages 71–94. Springer, 1998.
- [2] Charles Beattie, Joel Z Leibo, Denis Teplyashin, Tom Ward, Marcus Wainwright, Heinrich Küttler, Andrew Lefrancq, Simon Green, Víctor Valdés, Amir Sadik, et al. Deepmind lab. *arXiv preprint arXiv:1612.03801*, 2016.
- [3] Timothy EJ Behrens, Mark W Woolrich, Mark E Walton, and Matthew FS Rushworth. Learning the value of information in an uncertain world. *Nature neuroscience*, 10(9):1214–1221, 2007.
- [4] Marc G Bellemare, Yavar Naddaf, Joel Veness, and Michael Bowling. The arcade learning environment: An evaluation platform for general agents. *Journal of Artificial Intelligence Research*, 47:253–279, 2013.
- [5] Y Bengio, S Bengio, and J Cloutier. Learning a synaptic learning rule. In *Neural Networks, 1991., IJCNN-91-Seattle International Joint Conference on*, volume 2, pages 969–vol. IEEE, 1991.
- [6] Matthew Botvinick, Sam Ritter, Jane X Wang, Zeb Kurth-Nelson, Charles Blundell, and Demis Hassabis. Reinforcement learning, fast and slow. *Trends in cognitive sciences*, 23(5):408–422, 2019.
- [7] Tom B Brown, Benjamin Mann, Nick Ryder, Melanie Subbiah, Jared Kaplan, Prafulla Dhariwal, Arvind Neelakantan, Pranav Shyam, Girish Sastry, Amanda Askell, et al. Language models are few-shot learners. *arXiv preprint arXiv:2005.14165*, 2020.
- [8] Karl Cobbe, Chris Hesse, Jacob Hilton, and John Schulman. Leveraging procedural generation to benchmark reinforcement learning. In *International conference on machine learning*, pages 2048–2056. PMLR, 2020.
- [9] Karl Cobbe, Oleg Klimov, Chris Hesse, Taehoon Kim, and John Schulman. Quantifying generalization in reinforcement learning. In *International Conference on Machine Learning*, pages 1282–1289. PMLR, 2019.
- [10] Wojciech Marian Czarnecki, Razvan Pascanu, Simon Osindero, Siddhant M. Jayakumar, Grzegorz Swirszcz, and Max Jaderberg. Distilling policy distillation, 2019.
- [11] Ishita Dasgupta, Jane Wang, Silvia Chiappa, Jovana Mitrovic, Pedro Ortega, David Raposo, Edward Hughes, Peter Battaglia, Matthew Botvinick, and Zeb Kurth-Nelson. Causal reasoning from meta-reinforcement learning. *arXiv preprint arXiv:1901.08162*, 2019.
- [12] Nathaniel D Daw et al. Trial-by-trial data analysis using computational models. *Decision making, affect, and learning: Attention and performance XXIII*, 23(1), 2011.
- [13] Michael Dennis, Natasha Jaques, Eugene Vinitzky, Alexandre Bayen, Stuart Russell, Andrew Critch, and Sergey Levine. Emergent complexity and zero-shot transfer via unsupervised environment design. *arXiv preprint arXiv:2012.02096*, 2020.
- [14] Yan Duan, John Schulman, Xi Chen, Peter L. Bartlett, Ilya Sutskever, and Pieter Abbeel. RL<sup>2</sup>: Fast reinforcement learning via slow reinforcement learning. *arXiv preprint arXiv:1611.02779*, 2016.
- [15] Michael O Duff. Design for an optimal probe. In *Proceedings of the 20th International Conference on Machine Learning (ICML-03)*, pages 131–138, 2003.

- [16] Lasse Espeholt, Hubert Soyer, Remi Munos, Karen Simonyan, Volodymyr Mnih, Tom Ward, Yotam Doron, Vlad Firoiu, Tim Harley, Iain Dunning, et al. Impala: Scalable distributed deep-rl with importance weighted actor-learner architectures. *arXiv preprint arXiv:1802.01561*, 2018.
- [17] Simon Farrell and Stephan Lewandowsky. *Computational modeling of cognition and behavior*. Cambridge University Press, 2018.
- [18] Valerii Vadimovich Fedorov. *Theory of optimal experiments*. Elsevier, 2013.
- [19] Chelsea Finn, Pieter Abbeel, and Sergey Levine. Model-agnostic meta-learning for fast adaptation of deep networks. *arXiv preprint arXiv:1703.03400*, 2017.
- [20] Wilson S Geisler. Ideal observer analysis. *The visual neurosciences*, 10(7):12–12, 2003.
- [21] John C Gittins. Bandit processes and dynamic allocation indices. *Journal of the Royal Statistical Society. Series B (Methodological)*, pages 148–177, 1979.
- [22] Alison Gopnik, Clark Glymour, David M Sobel, Laura E Schulz, Tamar Kushnir, and David Danks. A theory of causal learning in children: causal maps and bayes nets. *Psychological review*, 111(1):3, 2004.
- [23] Erin Grant, Chelsea Finn, Sergey Levine, Trevor Darrell, and Thomas Griffiths. Recasting gradient-based meta-learning as hierarchical bayes. *arXiv preprint arXiv:1801.08930*, 2018.
- [24] Abhishek Gupta, Russell Mendonca, YuXuan Liu, Pieter Abbeel, and Sergey Levine. Meta-reinforcement learning of structured exploration strategies. *arXiv preprint arXiv:1802.07245*, 2018.
- [25] Felix Hill, Olivier Tieleman, Tamara von Glehn, Nathaniel Wong, Hamza Merzic, and Stephen Clark. Grounded language learning fast and slow. *arXiv preprint arXiv:2009.01719*, 2020.
- [26] Sepp Hochreiter and Jürgen Schmidhuber. Long short-term memory. *Neural Comput.*, 9(8):1735–1780, 1997.
- [27] Jan Humplik, Alexandre Galashov, Leonard Hasenclever, Pedro A Ortega, Yee Whye Teh, and Nicolas Heess. Meta reinforcement learning as task inference. *arXiv preprint arXiv:1905.06424*, 2019.
- [28] Max Jaderberg, Wojciech M Czarnecki, Iain Dunning, Luke Marris, Guy Lever, Antonio Garcia Castaneda, Charles Beattie, Neil C Rabinowitz, Ari S Morcos, Avraham Ruderman, et al. Human-level performance in 3d multiplayer games with population-based reinforcement learning. *Science*, 364(6443):859–865, 2019.
- [29] Max Jaderberg, Valentin Dalibard, Simon Osindero, Wojciech M. Czarnecki, Jeff Donahue, Ali Razavi, Oriol Vinyals, Tim Green, Iain Dunning, Karen Simonyan, Chrisantha Fernando, and Koray Kavukcuoglu. Population based training of neural networks, 2017.
- [30] Max Jaderberg, Volodymyr Mnih, Wojciech Marian Czarnecki, Tom Schaul, Joel Z Leibo, David Silver, and Koray Kavukcuoglu. Reinforcement learning with unsupervised auxiliary tasks. In *International Conference on Learning Representations*, 2017.
- [31] Matthew Johnson, Katja Hofmann, Tim Hutton, and David Bignell. The malmo platform for artificial intelligence experimentation. In *IJCAI*, pages 4246–4247. Citeseer, 2016.
- [32] Ashley L Juavinett, Jeffrey C Erlich, and Anne K Churchland. Decision-making behaviors: weighing ethology, complexity, and sensorimotor compatibility. *Current opinion in neurobiology*, 49:42–50, 2018.
- [33] Arthur Juliani, Vincent-Pierre Berges, Esh Vckay, Yuan Gao, Hunter Henry, Marwan Mattar, and Danny Lange. Unity: A general platform for intelligent agents. *arXiv preprint arXiv:1809.02627*, 2018.
- [34] Arthur Juliani, Ahmed Khalifa, Vincent-Pierre Berges, Jonathan Harper, Ervin Teng, Hunter Henry, Adam Crespi, Julian Togelius, and Danny Lange. Obstacle tower: A generalization challenge in vision, control, and planning. *arXiv preprint arXiv:1902.01378*, 2019.

- [35] Heinrich Küttler, Nantas Nardelli, Alexander H Miller, Roberta Raileanu, Marco Selvatici, Edward Grefenstette, and Tim Rocktäschel. The nethack learning environment. *arXiv preprint arXiv:2006.13760*, 2020.
- [36] Brenden M Lake, Tomer D Ullman, Joshua B Tenenbaum, and Samuel J Gershman. Building machines that learn and think like people. *Behavioral and brain sciences*, 40, 2017.
- [37] Evan Z Liu, Aditi Raghunathan, Percy Liang, and Chelsea Finn. Decoupling exploration and exploitation for meta-reinforcement learning without sacrifices. In *International Conference on Machine Learning*, pages 6925–6935. PMLR, 2021.
- [38] Russell Mendonca, Abhishek Gupta, Rosen Kralev, Pieter Abbeel, Sergey Levine, and Chelsea Finn. Guided meta-policy search. *arXiv preprint arXiv:1904.00956*, 2019.
- [39] Vladimir Mikulik, Grégoire Delétang, Tom McGrath, Tim Genewein, Miljan Martic, Shane Legg, and Pedro A Ortega. Meta-trained agents implement bayes-optimal agents. *arXiv preprint arXiv:2010.11223*, 2020.
- [40] Nikhil Mishra, Mostafa Rohaninejad, Xi Chen, and Pieter Abbeel. A simple neural attentive meta-learner. *International Conference on Learning Representations*, 2017.
- [41] Alex Nichol, Vicki Pfau, Christopher Hesse, Oleg Klimov, and John Schulman. Gotta learn fast: A new benchmark for generalization in rl. *arXiv preprint arXiv:1804.03720*, 2018.
- [42] OpenAI. Openai five. <https://blog.openai.com/openai-five/>, 2018.
- [43] Pedro A Ortega, Jane X Wang, Mark Rowland, Tim Genewein, Zeb Kurth-Nelson, Razvan Pascanu, Nicolas Heess, Joel Veness, Alex Pritzel, Pablo Sprechmann, et al. Meta-learning of sequential strategies. *arXiv preprint arXiv:1905.03030*, 2019.
- [44] Ian Osband, Yotam Doron, Matteo Hessel, John Aslanides, Eren Sezener, Andre Saraiva, Katrina McKinney, Tor Lattimore, Csaba Szepesvari, Satinder Singh, et al. Behaviour suite for reinforcement learning. *arXiv preprint arXiv:1908.03568*, 2019.
- [45] Emilio Parisotto, Jimmy Lei Ba, and Ruslan Salakhutdinov. Actor-mimic: Deep multitask and transfer reinforcement learning. *arXiv preprint arXiv:1511.06342*, 2015.
- [46] Emilio Parisotto, H Francis Song, Jack W Rae, Razvan Pascanu, Caglar Gulcehre, Siddhant M Jayakumar, Max Jaderberg, Raphael Lopez Kaufman, Aidan Clark, Seb Noury, et al. Stabilizing transformers for reinforcement learning. In *International Conference on Machine Learning*, 2019.
- [47] Kate Rakelly, Aurick Zhou, Chelsea Finn, Sergey Levine, and Deirdre Quillen. Efficient off-policy meta-reinforcement learning via probabilistic context variables. In *International conference on machine learning*, pages 5331–5340. PMLR, 2019.
- [48] Sebastian Risi and Julian Togelius. Increasing generality in machine learning through procedural content generation. *Nature Machine Intelligence*, 2(8):428–436, 2020.
- [49] Andrei A Rusu, Neil C Rabinowitz, Guillaume Desjardins, Hubert Soyer, James Kirkpatrick, Koray Kavukcuoglu, Razvan Pascanu, and Raia Hadsell. Progressive neural networks. *arXiv preprint arXiv:1606.04671*, 2016.
- [50] Adam Santoro, Sergey Bartunov, Matthew Botvinick, Daan Wierstra, and Timothy Lillicrap. Meta-learning with memory-augmented neural networks. In *International conference on machine learning*, pages 1842–1850, 2016.
- [51] Jürgen Schmidhuber. *Evolutionary principles in self-referential learning, or on learning how to learn: the meta-meta-... hook*. PhD thesis, Technische Universität München, 1987.
- [52] Simon Schmitt, Jonathan J Hudson, Augustin Zidek, Simon Osindero, Carl Doersch, Wojciech M Czarnecki, Joel Z Leibo, Heinrich Kuttler, Andrew Zisserman, Karen Simonyan, et al. Kickstarting deep reinforcement learning. *arXiv preprint arXiv:1803.03835*, 2018.
- [53] Julian Schrittwieser, Ioannis Antonoglou, Thomas Hubert, Karen Simonyan, Laurent Sifre, Simon Schmitt, Arthur Guez, Edward Lockhart, Demis Hassabis, Thore Graepel, et al. Mastering atari, go, chess and shogi by planning with a learned model. *Nature*, 588(7839):604–609, 2020.

- [54] Mohit Shridhar, Jesse Thomason, Daniel Gordon, Yonatan Bisk, Winson Han, Roozbeh Motlaghi, Luke Zettlemoyer, and Dieter Fox. Alfred: A benchmark for interpreting grounded instructions for everyday tasks. In *Proceedings of the IEEE/CVF conference on computer vision and pattern recognition*, pages 10740–10749, 2020.
- [55] H Francis Song, Abbas Abdolmaleki, Jost Tobias Springenberg, Aidan Clark, Hubert Soyer, Jack W Rae, Seb Noury, Arun Ahuja, Siqi Liu, Dhruva Tirumala, et al. V-mpo: on-policy maximum a posteriori policy optimization for discrete and continuous control. In *International Conference on Learning Representations*, 2019.
- [56] Bradly Stadie, Ge Yang, Rein Houthoofd, Peter Chen, Yan Duan, Yuhuai Wu, Pieter Abbeel, and Ilya Sutskever. The importance of sampling in meta-reinforcement learning. *Advances in Neural Information Processing Systems*, 31:9280–9290, 2018.
- [57] Bradly C Stadie, Ge Yang, Rein Houthoofd, Xi Chen, Yan Duan, Yuhuai Wu, Pieter Abbeel, and Ilya Sutskever. Some considerations on learning to explore via meta-reinforcement learning. *arXiv preprint arXiv:1803.01118*, 2018.
- [58] Richard S. Sutton and Andrew G. Barto. *Introduction to Reinforcement Learning*. MIT Press, 1998.
- [59] Joshua B Tenenbaum, Charles Kemp, Thomas L Griffiths, and Noah D Goodman. How to grow a mind: Statistics, structure, and abstraction. *science*, 331(6022):1279–1285, 2011.
- [60] Sebastian Thrun and Lorien Pratt. *Learning to learn*. Springer Science & Business Media, 1998.
- [61] Emanuel Todorov, Tom Erez, and Yuval Tassa. Mujoco: A physics engine for model-based control. In *2012 IEEE/RSJ International Conference on Intelligent Robots and Systems*, pages 5026–5033. IEEE, 2012.
- [62] Pedro A Tsividis, Joao Loula, Jake Burga, Nathan Foss, Andres Campero, Thomas Pouncy, Samuel J Gershman, and Joshua B Tenenbaum. Human-level reinforcement learning through theory-based modeling, exploration, and planning. *arXiv preprint arXiv:2107.12544*, 2021.
- [63] Saran Tunyasuvunakool, Alistair Muldal, Yotam Doron, Siqi Liu, Steven Bohez, Josh Merel, Tom Erez, Timothy Lillicrap, Nicolas Heess, and Yuval Tassa. dm\_control: Software and tasks for continuous control. *Software Impacts*, 6:100022, 2020.
- [64] Joaquin Vanschoren. Meta-learning. In *Automated Machine Learning*, pages 35–61. Springer, Cham, 2019.
- [65] Ashish Vaswani, Noam Shazeer, Niki Parmar, Jakob Uszkoreit, Llion Jones, Aidan N Gomez, Łukasz Kaiser, and Illia Polosukhin. Attention is all you need. In *Advances in neural information processing systems*, pages 5998–6008, 2017.
- [66] Oriol Vinyals, Igor Babuschkin, Wojciech M Czarnecki, Michaël Mathieu, Andrew Dudzik, Junyoung Chung, David H Choi, Richard Powell, Timo Ewalds, Petko Georgiev, et al. Grandmaster level in starcraft ii using multi-agent reinforcement learning. *Nature*, 575(7782):350–354, 2019.
- [67] Jane X Wang. Meta-learning in natural and artificial intelligence. *arXiv preprint arXiv:2011.13464*, 2020.
- [68] Jane X. Wang, Zeb Kurth-Nelson, Dhruva Tirumala, Hubert Soyer, Joel Z. Leibo, Rémi Munos, Charles Blundell, Dhharshan Kumaran, and Matthew Botvinick. Learning to reinforcement learn. In *Annual Meeting of the Cognitive Science Society*, 2016.
- [69] Marek Wydmuch, Michał Kempka, and Wojciech Jaśkowski. Vizdoom competitions: Playing doom from pixels. *IEEE Transactions on Games*, 2018.
- [70] Sirui Xie, Xiaojian Ma, Peiyu Yu, Yixin Zhu, Ying Nian Wu, and Song-Chun Zhu. Halma: Humanlike abstraction learning meets affordance in rapid problem solving. *arXiv preprint arXiv:2102.11344*, 2021.
- [71] Zhongwen Xu, Hado P van Hasselt, and David Silver. Meta-gradient reinforcement learning. *Advances in neural information processing systems*, 31:2396–2407, 2018.

- [72] Tianhe Yu, Deirdre Quillen, Zhanpeng He, Ryan Julian, Karol Hausman, Chelsea Finn, and Sergey Levine. Meta-world: A benchmark and evaluation for multi-task and meta reinforcement learning. In *Conference on Robot Learning*, pages 1094–1100. PMLR, 2020.
- [73] Luisa Zintgraf, Kyriacos Shiarlis, Maximilian Igl, Sebastian Schulze, Yarin Gal, Katja Hofmann, and Shimon Whiteson. Varibad: A very good method for bayes-adaptive deep rl via meta-learning. *arXiv preprint arXiv:1910.08348*, 2019.

## Checklist

1. For all authors...
  - (a) Do the main claims made in the abstract and introduction accurately reflect the paper’s contributions and scope? [Yes]
  - (b) Did you describe the limitations of your work? [Yes] See section 5.
  - (c) Did you discuss any potential negative societal impacts of your work? [Yes] As part of our paper, we are providing an open-source benchmark and analysis tools for meta-RL researchers, which should overall benefit the community. We don’t anticipate any negative societal impacts from this work, but if reviewers see any potential issues, we are happy to discuss them.
  - (d) Have you read the ethics review guidelines and ensured that your paper conforms to them? [Yes]
2. If you are including theoretical results...
  - (a) Did you state the full set of assumptions of all theoretical results? [N/A]
  - (b) Did you include complete proofs of all theoretical results? [N/A]
3. If you ran experiments (e.g. for benchmarks)...
  - (a) Did you include the code, data, and instructions needed to reproduce the main experimental results (either in the supplemental material or as a URL)? [Yes] We have already open-sourced the code and data to the public, and have included the link in the submission.
  - (b) Did you specify all the training details (e.g., data splits, hyperparameters, how they were chosen)? [Yes] See section B.1 in the appendix.
  - (c) Did you report error bars (e.g., with respect to the random seed after running experiments multiple times)? [Yes] All replicas from random seeds are reported as individual dots on plots, or as individual performance lines, to give indications of variability over different runs. This gives more information than error bars because error bars make assumptions about normality.
  - (d) Did you include the total amount of compute and the type of resources used (e.g., type of GPUs, internal cluster, or cloud provider)? [Yes] See section B.1 in the appendix.
4. If you are using existing assets (e.g., code, data, models) or curating/releasing new assets...
  - (a) If your work uses existing assets, did you cite the creators? [Yes] We cite the creators of VMPO, Impala, and the Unity agent environment which are the assets used by this work.
  - (b) Did you mention the license of the assets? [Yes] The licenses of the different assets used for the Unity agent environments are provided with the binaries of the environment in a NOTICES file. The code itself does not directly include any existing assets.
  - (c) Did you include any new assets either in the supplemental material or as a URL? [Yes] We provide the environment along with analysis code.
  - (d) Did you discuss whether and how consent was obtained from people whose data you’re using/curating? [N/A]
  - (e) Did you discuss whether the data you are using/curating contains personally identifiable information or offensive content? [N/A]
5. If you used crowdsourcing or conducted research with human subjects...
  - (a) Did you include the full text of instructions given to participants and screenshots, if applicable? [N/A]
  - (b) Did you describe any potential participant risks, with links to Institutional Review Board (IRB) approvals, if applicable? [N/A]
  - (c) Did you include the estimated hourly wage paid to participants and the total amount spent on participant compensation? [N/A]

## A Alchemy mechanics

### A.1 The chemistry

We consider three perceptual features along which stones can vary: size, color, and shape. Potions are able to change stone perceptual features, but how a specific potion can affect a particular stone’s appearance is determined by the stone’s (unobserved) latent state  $\mathbf{c}$ . Each potion deterministically transforms stones according to a hidden, underlying transition graph sampled from the set of all connected graphs formed by the edges of a cube (see Figure 7a). The corners of the cube represent different latent states, defined by a 3-dimensional coordinate  $\mathbf{c} \in \{-1, 1\}^3$ . Potion effects align with one axis and direction of the cube, such that one of the coordinates  $\mathbf{c}$  is modified from -1 to 1 or 1 to -1. In equations:

$$\mathbf{c} = \mathbf{c} + 2\mathbf{p}\mathbb{1}_{(\mathbf{c}, \mathbf{c}+2\mathbf{p}) \in G}(\mathbf{c}) \quad (1)$$

where  $\mathbf{p} \in \mathcal{P}$  is the potion effect  $\mathcal{P} := \{\mathbf{e}^{(0)}, \mathbf{e}^{(1)}, \mathbf{e}^{(2)}, -\mathbf{e}^{(0)}, -\mathbf{e}^{(1)}, -\mathbf{e}^{(2)}\}$  where  $\mathbf{e}^{(i)}$  is the  $i^{\text{th}}$  basis vector and  $G$  is the set of edges which can be traversed in the graph.

The latent state of the stone also determines its reward value  $R \in \{-3, -1, 1, 15\}$ , which can be observed via the brightness of the reward indicator (square light) on the stone:

$$R(\mathbf{c}) = \begin{cases} 15, & \text{if } \sum_i c_i = 3 \\ \sum_i c_i, & \text{else.} \end{cases} \quad (2)$$

The agent only receives a reward for a stone if that stone is successfully placed within the cauldron by the end of the trial, which removes the stone from the game.

The latent coordinates  $\mathbf{c}$  are mapped into the stone perceptual feature space to determine the appearance of the stone. We call this linear mapping the stone map or  $S$  and define it as  $S: \{-1, 1\}^3 \rightarrow \{-1, 0, 1\}^3$ :

$$S(\mathbf{c}) = \mathbf{S}_{\text{rotate}}\mathbf{S}_{\text{reflect}}\mathbf{c} \quad (3)$$

where  $\mathbf{S}_{\text{rotate}}$  denotes possible rotation around 1 axis and rescaling. Formally:  $\mathbf{S}_{\text{rotate}} \sim U(\{\mathbf{I}_3, \overline{R}_x(45^\circ), \overline{R}_y(45^\circ), \overline{R}_z(45^\circ)\})$ , where  $\mathbf{I}$  is the identity matrix, and  $\overline{R}_i(\theta)$  denotes an anti-clockwise rotation transform around axis  $i$  by  $\theta = 45^\circ$ , followed by scaling by  $\frac{\sqrt{2}}{2}$  on all other axes, in order to normalize values to be in  $\{-1, 0, 1\}$ .  $\mathbf{S}_{\text{reflect}}$  denotes reflection in the  $x$ ,  $y$  and  $z$  axes:  $\mathbf{S}_{\text{reflect}} = \text{diag}(\mathbf{s})$  for  $\mathbf{s} \sim U(\{-1, 1\}^3)$ .

The potion effect  $\mathbf{p}$  is mapped to a potion color by first applying a linear mapping and then using a fixed look-up table to find the color. We call this linear mapping the potion map  $P: \mathcal{P} \rightarrow \mathcal{P}$ .

$$P(\mathbf{p}) = \mathbf{P}_{\text{reflect}}\mathbf{P}_{\text{permute}}\mathbf{p} \quad (4)$$

where  $\mathbf{P}_{\text{reflect}}$  is drawn from the same distribution as  $\mathbf{S}_{\text{reflect}}$  and  $\mathbf{P}_{\text{permute}}$  is a 3x3 permutation matrix i.e. a matrix of the form  $[\mathbf{e}^{(\pi(0))}, \mathbf{e}^{(\pi(1))}, \mathbf{e}^{(\pi(2))}]^T$ ,  $\pi \sim U(\text{Sym}(\{0, 1, 2\}))$  where  $\text{Sym}(\{0, 1, 2\})$  is the set of permutations of  $\{0, 1, 2\}$ .

The directly observable potion colors are then assigned according to:

$$P_{\text{color}} = \begin{cases} (\mathbf{e}^{(0)}, -\mathbf{e}^{(0)}) \rightarrow (\text{green}, \text{red}) \\ (\mathbf{e}^{(1)}, -\mathbf{e}^{(1)}) \rightarrow (\text{yellow}, \text{orange}) \\ (\mathbf{e}^{(2)}, -\mathbf{e}^{(2)}) \rightarrow (\text{turquoise}, \text{pink}) \end{cases} \quad (5)$$

Note that this implies that potion colors come in pairs so that, for example, the red potion always has the opposite effect to the green potion, though that effect may be on color, size, or shape, depending on the particular chemistry of that episode. It can also have an effect on two of those three perceptual features simultaneously in the case where  $\mathbf{S}_{\text{rotate}} \neq \mathbf{I}_3$ . This color pairing of potions is consistent across all samples of the task, constituting a feature of Alchemy which can be meta-learned over

many episodes. Importantly, due to the potion map  $P$ , the potion effects  $\mathbf{p}$  in each episode must be discovered by experimentation.

$G$  is determined by sampling a graph topology (Figure 7d), which determines which potion effects are possible. Potions only have effects if certain preconditions on the stone latent state are met, which constitute ‘bottlenecks’ (darker edges in Figure 7d). Each graph consists of the edges of the cube which meet the graph’s set of preconditions. Each precondition says that an edge parallel to axis  $i$  exists only if its value on axis  $j$  is  $a$  where  $j \neq i$  and  $a \in \{-1, 1\}$ . The more preconditions, the fewer edges the graph has.

Only sets of preconditions which generate a connected graph are allowed. We denote the set of connected graphs with preconditions of this form  $\mathbb{G}$ . Note that this is smaller than the set of all connected graphs, as a single precondition can rule out 1 or 2 edges of the cube. As with the potion color pairs, this structure is consistent across all samples and may be meta-learned.

We find that the maximum number of preconditions for any graph  $G \in \mathbb{G}$  is 3. We define  $\mathbb{G}^n := \{G \in \mathbb{G} | N(G) = n\}$  where  $N(G)$  is the number of preconditions in  $G$ . The sampling distribution is  $n \sim U(0, 3)$ ,  $G \sim U(\mathbb{G}^n)$ . Of course, there is only one graph with 0 preconditions and many graphs with 1, 2, or 3 preconditions so the graph with 0 preconditions is the most common and is sampled 25% of the time.

A ‘chemistry’ is a random sampling of all variables  $\{G, \mathbf{P}_{\text{permute}}, \mathbf{P}_{\text{reflect}}, \mathbf{S}_{\text{reflect}}, \mathbf{S}_{\text{rotate}}\}$  (subject to the constraint rules described above), which is held constant for an episode (Figure 6). Given all of the possible permutations, we calculate that there are 167,424 total chemistries that can be sampled.

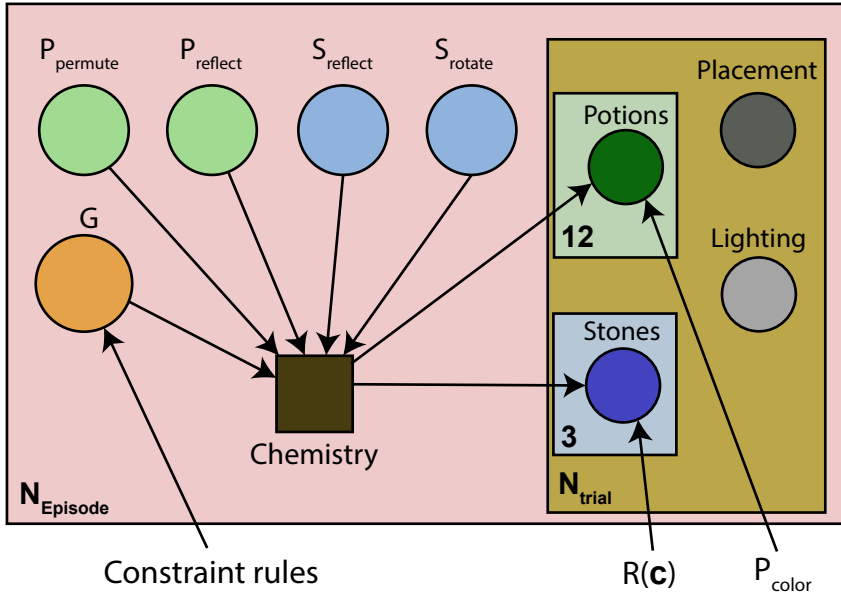


Figure 6: The generative process for sampling a new task, in plate notation. Constraint rules  $\mathbb{G}$ ,  $P_{\text{color}}$ , and  $R(\mathbf{c})$  are fixed for all episodes (see Section A.1). Every episode, a set  $\{G, \mathbf{P}_{\text{permute}}, \mathbf{P}_{\text{reflect}}, \mathbf{S}_{\text{reflect}}, \mathbf{S}_{\text{rotate}}\}$  is sampled to form a new chemistry. Conditioned on this chemistry, for each of  $N_{\text{trial}} = 10$  trials,  $N_s = 3$  stones and  $N_p = 12$  potions are sampled, as well as random placement and lighting conditions, to form the perceptual observation for the agent. For clarity, the above visualization omits parameters for normal or uniform distributions over variables (such as lighting and placement of stones/potions on the table).

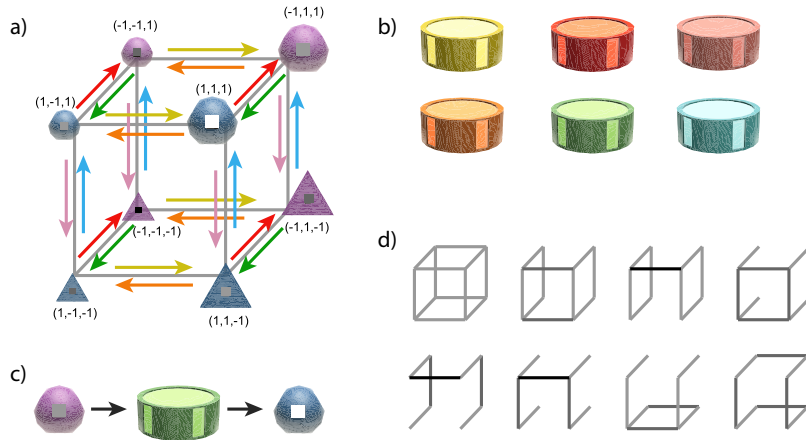


Figure 7: a) Depiction of an example chemistry sampled from Alchemy, in which the perceptual features happen to be axis-aligned with the latent feature coordinates (listed beside the stones). Stones transform according to a hidden transition structure, with edges corresponding to the application of corresponding potions, as seen in b). c) For example, applying the green potion to the large purple stone transforms it into a large blue stone, and also increases its value (indicated by the square in center of stone becoming white). d) The possible graph topologies for stone transformation. Darker edges indicate ‘bottlenecks’, which are transitions that are only possible from certain stone latent states. In topologies with bottlenecks, more potions are often required to reach the highest value stone. If the criteria for stone states are not met, then the potion will have no effect (e.g. if topology (v) has been sampled, the yellow potion in the example given in (a) will have no effect on the small purple round stone). Note that we can apply reflections and rotations on these topologies, yielding a total of 109 configurations.

## A.2 Episode structure

Episodes end at the end of 10 trials, with a fixed number of steps per trial. There are 20 steps per trial for symbolic Alchemy (200 for the entire episode), and 1800 frames (18000 for the entire episode, at a frame rate of 30 fps) for 3D Alchemy.

The chemistry is procedurally generated at the beginning of every episode, and held constant for the entire episode. Conditioned on this chemistry, stones and potions are sampled at the beginning of every trial, with different placement and lighting (in 3D Alchemy).

## **B Training details**

### **B.1 Compute and hyperparameters**

For each experiment running VMPO on the symbolic Alchemy environment we used 460 TPUv2 core hours and 1.4 million CPU core hours at 2.4GHz. For each experiment running VMPO on the full 3d Alchemy environment we used 2500 TPUv3 core hours and 1.7 million CPU core hours at 2.4GHz. For each experiment running IMPALA on the full 3d Alchemy environment we used 560 TPUv3 core hours and 200 thousand CPU core hours at 2.4GHz. However, please note that VMPO and IMPALA are general purpose deep RL agents designed for completely different tasks, and so it is not surprising that they are not efficient at Alchemy. We expect that new agents designed to solve the meta-learning challenge proposed by Alchemy would be able to be much more data efficient.

Coarse hyperparameter searches were conducted in order to balance resource constraints against the complexity of the task, doing sweeps (2-3 values) over learning rate and agent-specific hyperparameters such as the epsilon temperature and target update period for VMPO. Default hyperparameters were taken either from the original VMPO [46, 55] and Impala [16] papers, or swept in consultation with the authors, based on their best estimate of what could work for Alchemy.

Table 2: Architecture and hyperparameters for VMPO.

SETTING	VALUE
IMAGE RESOLUTION:	96x72x3
NUMBER OF ACTION REPEATS:	4
AGENT DISCOUNT:	0.99
RESNET NUM CHANNELS:	64, 128, 128
TRXL MLP SIZE:	256
TRXL NUMBER OF LAYERS:	6
TRXL NUMBER OF HEADS:	8
TRXL KEY/VALUE SIZE:	32
$\epsilon_\eta$ :	0.5
$\epsilon_\alpha$ :	0.001
$T_{\text{TARGET}}$ :	100
$\beta_\pi$ :	1.0
$\beta_V$ :	1.0
$\beta_{\text{PIXEL CONTROL}}$ :	0.001
$\beta_{\text{KICKSTARTING}}$ :	10.0
$\beta_{\text{STONE}}$ :	2.4
$\beta_{\text{POTION}}$ :	0.6
$\beta_{\text{CHEMISTRY}}$ :	10.0

Table 3: Architecture and hyperparameters for Impala.

SETTING	VALUE
IMAGE RESOLUTION:	96x72x3
NUMBER OF ACTION REPEATS:	4
AGENT DISCOUNT:	0.99
LEARNING RATE:	0.00033
RESNET NUM CHANNELS:	16, 32, 32
LSTM HIDDEN UNITS:	256
$\beta_\pi$ :	1.0
$\beta_V$ :	0.5
$\beta_{\text{ENTROPY}}$ :	0.001
$\beta_{\text{PIXEL CONTROL}}$ :	0.2
$\beta_{\text{KICKSTARTING}}$ :	8.0

---

**Algorithm 1** Ideal Observer

---

**Input:** stones  $s$ , potions  $p$ , belief state  $b$   
Initialise rewards = { }  
**for all**  $s_i \in s$  **do**  
  **for all**  $p_j \in p$  **do**  
     $s_{\text{poss}}, p_{\text{poss}}, b_{\text{poss}}, b_{\text{probs}} = \text{simulate use potion}(s, p, s_i, p_j, b)$   
     $r = 0$   
    **for all**  $s', p', b', prob \in s_{\text{poss}}, p_{\text{poss}}, b_{\text{poss}}, b_{\text{probs}}$  **do**  
       $r = r + prob * \text{Ideal Observer}(s', p', b')$   
    **end for**  
    rewards[ $s_i, p_j$ ] =  $r$   
  **end for**  
   $s', r = \text{simulate use cauldron}(s, s_i)$   
  rewards[ $s_i, \text{cauldron}$ ] =  $r + \text{Ideal Observer}(s', p, b)$   
**end for**  
**return** argmax(rewards)

---

---

**Algorithm 2** Oracle

---

**Input:** stones  $s$ , potions  $p$ , chemistry  $c$   
Initialise rewards = { }  
**for all**  $s_i \in s$  **do**  
  **for all**  $p_j \in p$  **do**  
     $s', p' = \text{simulate use potion}(s, p, s_i, p_j, c)$   
    rewards[ $s_i, p_j$ ] = Oracle( $s', p', c$ )  
  **end for**  
   $s', r = \text{simulate use cauldron}(s, s_i)$   
  rewards[ $s_i, \text{cauldron}$ ] =  $r + \text{Oracle}(s', p, c)$   
**end for**  
**return** argmax(rewards)

---

## B.2 Auxiliary task losses

Auxiliary prediction tasks include: 1) predicting the number of stones currently present that possess each possible perceptual feature (e.g. small size, blue color etc), 2) predicting the number of potions of each color, or 3) predicting the ground truth chemistry. Auxiliary tasks contribute additional losses which are summed with the standard RL losses, weighted by coefficients ( $\beta_{\text{stone}} = 2.4$ ,  $\beta_{\text{potion}} = 0.6$ ,  $\beta_{\text{chem}} = 10.0$ ). These hyperparameters were determined by roughly balancing the gradient norms of variables which contributed to all losses. All prediction tasks use an MLP head, (1) and (2) use an L2 regression loss while (3) uses a cross entropy loss. Prediction tasks (1) and (2) were always done in conjunction and are collectively referred to as ‘Predict: Features’, while (3) is referred to as ‘Predict: Chemistry’ in the results.

The MLP for 1) has 128x128x13 units where the final layer represents 3 predictions for each perceptual feature value e.g. the number of small stones, medium stones, large stones and 4 predictions for the brightness of the reward indicator. The MLP for 2) has 128x128x6 units where the final layer represents 1 prediction for the number of potions of each possible color. 3) is predicted with an MLP with a sigmoid cross entropy loss and has size 256x128x28 where the final layer represents predictions of the symbolic representations of the graph and mappings ( $\mathbf{S}_{\text{rotate}}, \mathbf{S}_{\text{reflect}}, \mathbf{P}_{\text{reflect}}, \mathbf{P}_{\text{permute}}, G$ ). More precisely,  $\mathbf{S}_{\text{rotate}}$  is represented by a 4 dimensional 1-hot,  $\mathbf{S}_{\text{reflect}}$  and  $\mathbf{P}_{\text{reflect}}$  are represented by 3 dimensional vectors with a 1 in the  $i^{\text{th}}$  element denoting reflection in axis  $i$ ,  $\mathbf{P}_{\text{permute}}$  is represented by a 6 dimensional 1-hot and  $G$  is represented by a 12-dimensional vector for the 12 edges of the cube with a 1 if the corresponding edge exists and a 0 otherwise.

---

**Algorithm 3** Random heuristic

---

```
Input: stones  $s$ , potions  $p$ , threshold  $t$   
 $s_i = \text{random choice}(s)$   
if  $\text{reward}(s_i) > t$  or ( $\text{reward}(s_i) > 0$  and  $\text{empty}(p)$ ) then  
    return  $s_i$ , cauldron  
end if  
 $p_i = \text{random choice}(p)$   
return  $s_i, p_i$ 
```

---

## C Additional results

Training curves show that VMPO agents train faster in the symbolic version of Alchemy vs the 3D version (Figures 8 and 9), even though agents are kickstarted in 3D.

As seen in Figure 9, the auxiliary task of predicting features appears much more beneficial than predicting the ground truth chemistry, the latter leading to slower training and more variability across seeds. We hypothesize that this is because predicting the underlying chemistry is possibly as difficult as simply performing well on the task, while predicting simple feature statistics is tractable, useful, and leads to more generalizable knowledge.

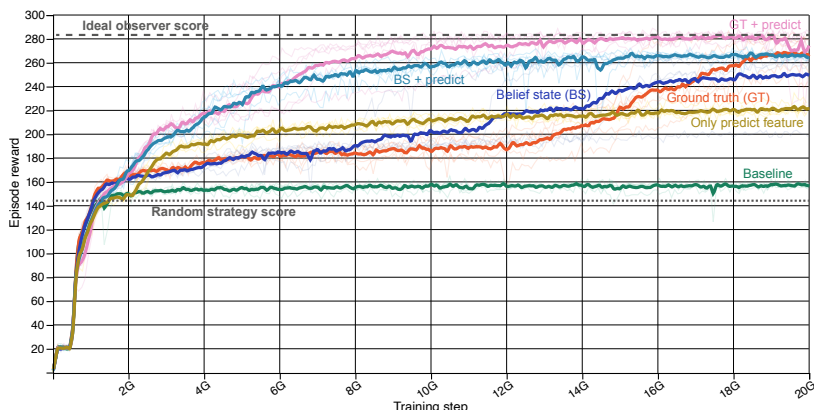


Figure 8: 3D with symbolic input training. Data are smoothed by bucketing and averaging over 2M steps per bucket (for a total of 1000 points). Thin lines indicate individual replicas (5 per condition).

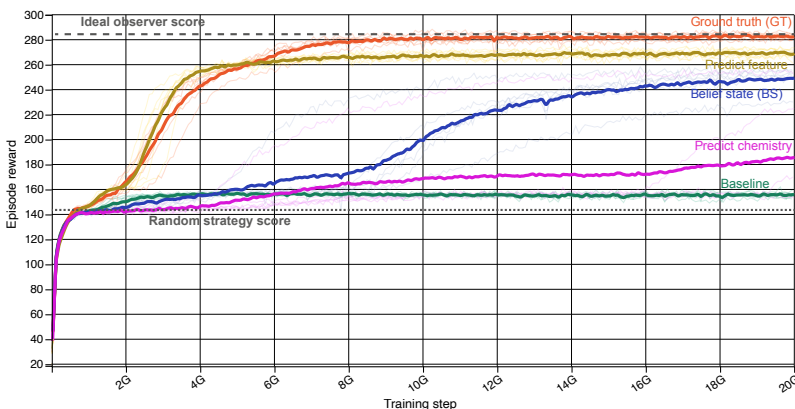


Figure 9: Symbolic alchemy training. Data are smoothed by bucketing and averaging over 2M steps per bucket (for a total of 1000 points). Thin lines indicate individual replicas (5 per condition).

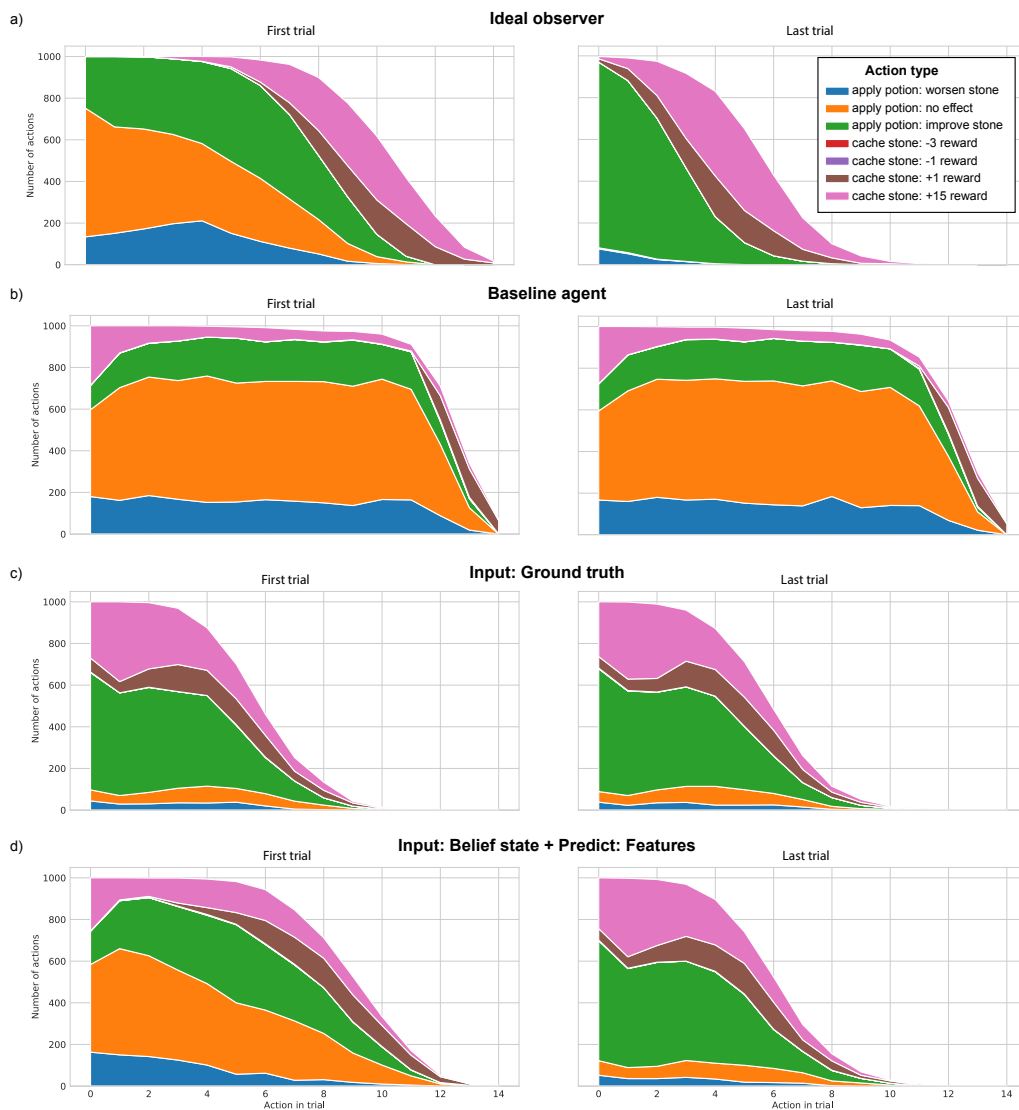


Figure 10: Comparing action types throughout trial in 3D alchemy, for a) ideal observer, b) baseline agent, c) agent with ground truth information as input, and d) agent with belief state as input and feature prediction auxiliary task. All agents include the symbolic observations as input. The ideal strategy is to in trial 1 perform a lot of exploratory actions (yielding actions that lead to no effect on the stone), but then in later trials perform only actions that change the value of the stone. Unlike the ideal observer, the baseline agent (b) and agent with ground truth input (c) display no change between the first and last trials, indicating an inability to adapt strategies (exploration vs exploitation) throughout the course of the episode.

## D Licenses and documentation

The Alchemy environment and analysis tools can be found at [https://github.com/deepmind/dm\\_alchemy](https://github.com/deepmind/dm_alchemy) and are released under the Apache License 2.0. Further licensing details and all documentation, including a colab tutorial, can be found at this repository.

Code will be updated and maintained by a subset of the authors with support from DeepMind and contributions from the community.